Biochemical and Biophysical Research Communications 459 (2015) 87–93

Contents lists available at ScienceDirect

Biochemical and Biophysical Research Communications

journal homepage: www.elsevier.com/locate/ybbrc

Biophysical characterization of interactions between the C-termini of peripheral nerve claudins and the PDZ_1 domain of zonula occludens

Jiawen Wu [a, f], Dungeng Peng [a], Yang Zhang [a], Zhenwei Lu [b], Markus Voehler [c], Charles R. Sanders [b, c], Jun Li [a, d, e, *]

[a] Department of Neurology, Vanderbilt University School of Medicine, USA
[b] Department of Biochemistry, Vanderbilt University School of Medicine, USA
[c] Center for Structural Biology, Vanderbilt University, USA
[d] Tennessee Valley Healthcare System (TVHS), Nashville, VA, USA
[e] Center for Human Genetics Research, Vanderbilt University School of Medicine, USA
[f] Anhui University of Chinese Medicine, Hefei, Anhui, China

ARTICLE INFO

Article history:
Received 4 February 2015
Available online 21 February 2015

Keywords:
ZO1, zonula occludens-1
ZO2, zonula occludens-2
PNS, peripheral nervous system
Myelin junction
Myelin permeability
PMP22, peripheral myelin protein-22

ABSTRACT

Our recent study has shown that cellular junctions in myelin and in the epi-/perineruium that encase nerve fibers regulate the permeability of the peripheral nerves. This permeability may affect propagation of the action potential. Direct interactions between the PDZ_1 domain of zonula occludens (ZO_1 or ZO_2) and the C-termini of claudins are known to be crucial for the formation of tight junctions. Using the purified PDZ_1 domain of ZO_2 and a variety of C-terminal mutants of peripheral nerve claudins (claudin-1, claudin-2, claudin-3, claudin-5 in epi-/perineurium; claudin-19 in myelin), we have utilized NMR spectroscopy to determine specific roles of the 3 C-terminal claudin residues (position −2, −1, 0) for their interactions with PDZ_1 of ZO_2. In contrast to the canonical model that emphasizes the importance of residues at the −2 and 0 positions, our results demonstrate that, for peripheral nerve claudins, the residue at position −1 plays a critical role in association with PDZ_1, while the side-chain of residue 0 plays a significant but lesser role. Surprisingly, claudin-19, the most abundant claudin in myelin, exhibited no binding to ZO_2. These findings reveal that the binding mechanism of claudin/ZO in epi-/perineurium is distinct from the canonical interactions between non-ZO PDZ-containing proteins with their ligands. This observation provides the molecular basis for a strategy to develop drugs that target tight junctions in the epi-/perineurium of peripheral nerves.

Published by Elsevier Inc.

1. Introduction

Our recent work has shown that peripheral nerve conduction may be affected by changing nerve permeability through junctions in myelin and epi-/perineurium, such as tight junctions and adherens junctions [5]. These junctions share a similar molecular framework (Fig. 1A). Transmembrane proteins such as claudins in tight junctions establish “trans-adhesion” between opposing membranes. They oligomerize in “cis” within the same membrane and interact with a variety cytosolic adaptor proteins, such as zonula occludens (ZO_1 or ZO_2), which also complex with the sub-membrane actin network for junction stabilization [7].

In tight junctions, the first PDZ domain (PDZ_1) of ZO_1, ZO_2 and ZO_3 has been reported to directly interact with the short C-termini of claudin-1, claudin-2 and claudin-3 [9]. In general, binding requirements between PDZ domain and its ligand protein mainly involve the final 3 amino acids (residues at position 0, −1, and −2) of the ligand C-terminus (Fig. 1B, C), and are independent of the overall structure of the ligand proteins. Specifically, the carboxyl and side chain of the residue at the position 0 plus the side chain of the residue at the position −2 are thought to play critical roles in rendering affinity and specificity of the binding. This structural conservation makes it an attractive molecular target for drug development [4]. However, specific requirements of C-terminal residues have not been studied in the binding between PDZ_1 of ZOs and the claudins found in the peripheral nerve system (PNS).

* Corresponding author. Department of Neurology, Vanderbilt University, 1161, 21st Avenue South, Nashville, TN 37232, USA.
E-mail address: jun.li.2@vanderbilt.edu (J. Li).

http://dx.doi.org/10.1016/j.bbrc.2015.02.075
0006-291X/Published by Elsevier Inc.

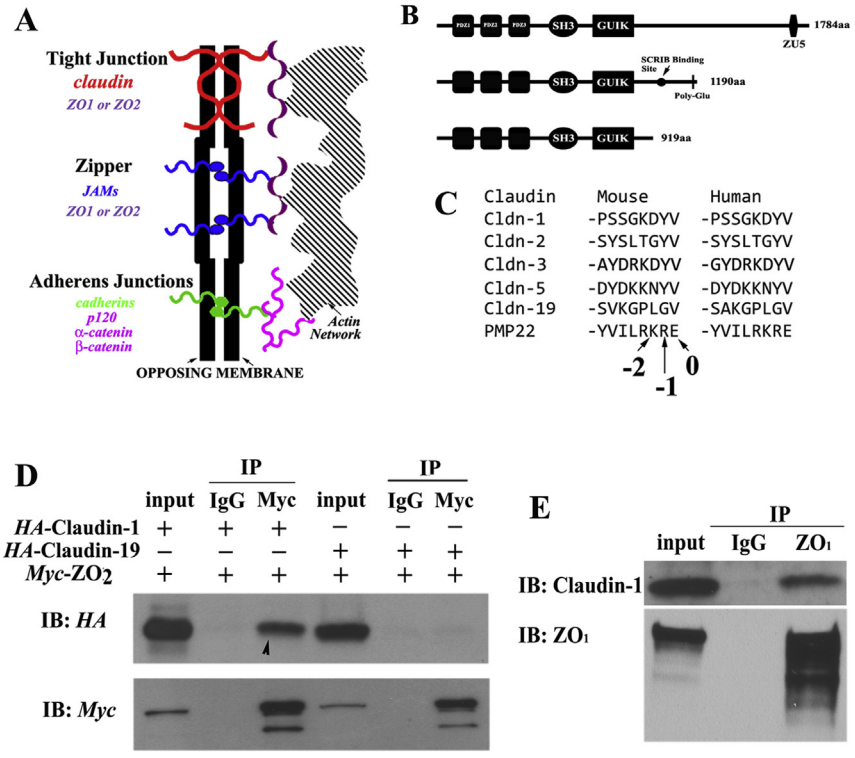

Fig. 1. A. This diagram shows a general molecular framework in different junctions. Transmembrane proteins can interact to provide "*trans*-adhesion" between opposing membranes. Through a variety of adaptor proteins, such as $ZO_{1,2}$ or catenins these junction protein complexes are stabilized by a sub-membrane actin network. **B**. A diagram shows domains in ZO_1, ZO_2 and ZO_3. GUIK = guanylate kinase-like domain. **C**. Listed are amino acid sequences of peripheral nerve claudin C-termini. Notice that the positions for the final 3 residues are referred to as positions −2, −1 and 0. **D**. Co-IP was performed in HEK293 cells and detected an interaction between claudin-1 and ZO_2 (arrowhead). The co-IP experiment failed to detect any interaction between claudin-19 and ZO_2. Note that claudin-1, claudin-19 and ZO_2 were all expressed in full length. Amount of proteins loaded in the first and second input lane was 7.5 μg and 15 μg respectively. **E**. Human claudin1 was transfected into rat Schwann cells. Ten percent of cell lysates was loaded as the input. Lysates were immunoprecipitated with ZO_1 antibody. The precipitated proteins were detected by immunoblotting with Claudin-1 or ZO_1 antibodies (IP lanes). IB = immunoblting; IP = immunoprecipitation.

Tight junctions are the key barrier blocking access through epineurium/myelin to the axons of the PNS. Given that only a limited number of claudins (claudin-1, claudin-2, claudin-3, claudin-5, claudin-19) and ZOs (ZO_1, ZO_2) are expressed in myelinating Schwann cells and epi-/perineurial cells [5,12,13], specific drug targeting in the PNS tight junctions may be feasible. In the present study, we utilize NMR spectroscopy to probe the PDZ_1 structure of $ZO_2$and its formation of complexes with the C-termini of peripheral nerve claudins.

2. Methods

2.1. Co-immunoprecipitation (co-IP):

Plasmids. All plasmids contained human cDNA clones. HA-tagged PMP22, ZO_1 and Myc-tagged ZO_2 plasmids were from Genecopoeia or Origene. A non-tagged claudin-1 plasmid (from Thermo) was sub-cloned into pCMV6-AN-HA to encode expression of HA-tagged claudin-1. The accuracy of these plasmids was verified by DNA sequencing.

Transfection and co-IP: Plasmids were transfected into HEK293a or Schwann cells using Effectene (Qiagen). Supernatants from the transfected cell lysates and corresponding antibodies were used for co-IP, and were incubated with protein-G agarose beads (Life Technologies). Proteins were boiled off the beads in 2 × SDS loading buffer and separated on SDS–PAGE for Western blot analysis. The following antibodies were used: ZO_1 (Invitrogen #61-7300 for IP; #339100 for Western blot), claudin-1 (Invitrogen, #37-4900).

2.2. Plasmids to express and purify proteins for NMR study

DNA encoding the PDZ_1 of mouse ZO_2 (NCBI: NP_035727.2) was amplified from a mouse brain cDNA library (Open Biosystems, #LMM 1206) using primers: sense: 5′-CGACTACATATGATGGAGG AGGTGATATGGGAGCAG-3′ and anti-sense: 5′-TATCTCGAGTCAGGG CCACCTGAACCTTCCGGGGT-3'. The cDNA was sub-cloned into the Nde1/Xho1 sites of the pET28a(+) vector to express the mouse ZO_2 protein (M-ZO_2PDZ_1) fused with an N-terminal His-tag. The construct was verified by DNA sequencing.

The recombinant plasmids harboring the M-ZO_2PDZ_1 cDNA were transformed into *E. coli* BL21(DE3) cells. Protein expression was induced by 0.5 mM isopropyl β-d-thiogalactopyranoside (IPTG). M-ZO_2PDZ_1 proteins were labeled with ^{15}N- or $^{15}N/^{13}C$ by growing bacteria in M9 medium using $^{15}NH_4Cl$ (2.0 g/l) and $^{13}C_6$-glucose (2.0 g/l). Cells were lysed by sonication. M-ZO_2PDZ_1 was purified using a Ni-NTA column (Qiagen). The His-tag was removed by thrombin in a buffer consisting of 50 mM Tris (pH8.0), 150 mM NaCl, 2.5 mM $CaCl_2$ and 0.1% β-mercaptoethanol. The recovered M-ZO_2PDZ_1 was exchanged into buffer-A (50 mM phosphate buffer, 50 mM NaCl, 0.2 mM EDTA, pH 5.2) using a Millipore centrifugal filter (<3 kDa). The purity of M-ZO_2PDZ_1 was confirmed by Tricine-SDS-PAGE (12%, w/v), and the concentration was measured using BCA kits (Pierce).

2.3. NMR spectroscopy

The purified proteins were dissolved to a final concentration of 0.3–0.5 mM in buffer-A with a 95% H_2O/5% D_2O mixture. All NMR spectra were collected at 298 K using a Bruker AV-III spectrometer at 600 MHz and CPTCI probe. $^{1}H-^{15}N$ HSQC spectra were acquired on ^{15}N-labeled samples. A $^{15}N/^{13}C$-labeled sample was used to collect triple resonance spectra for backbone resonance assignments and secondary structure determination. NMR spectra were processed using NMRPipe [2] or TopSpin (Bruker Biospin Inc., MA), and analyzed by Sparky software (Goddard and Kneller, V3.113, 2006, University of California).

2.4. NMR titrations

Unmodified peptides (50 mM; purity>95%; Genscript) were added to 180 μl ^{15}N-labeled ZO_2PDZ_1 (0.1 mM in Buffer-A). The total sample dilution over the course of a titration was no more than 10%. For each titration point, a 2D $^{1}H-^{15}N$ HSQC spectrum was acquired. Composite chemical shift perturbation was calculated using $\Delta\delta(ppm) = \{[\Delta\delta(HN)]^2 + [0.17\cdot\Delta\delta(N)]^2\}^{1/2}$ [17], in which $\Delta\delta$HN and $\Delta\delta$N were the titration-induced proton and nitrogen chemical shift changes. The final molar ratios between the peptides and ^{15}N-labeled M-ZO_2PDZ_1 were in all cases ≥12:1.

Determination of dissociation constants: please see Supplementary Fig. 1.

3. Results

3.1. Verification of interactions between claudins and ZO_2 by co-IP

Studies have shown direct interactions between claudins (claudin1, claudin-2 and claudin-3) and ZOs (ZO-1, ZO2 and ZO3) by GST pull-down assay. The interaction depends on the YV-motif at the C-termini of claudins [9]. We verified the interaction between claudin-1 and ZO_2 using co-IP. Claudin-1 and ZO_2 were co-expressed in HEK293a cells. Antibodies against the HA-tag of claudin-1 were able to pull down its binding partner of ZO_2 (arrowhead in Fig. 1D). In contrast, no interaction was detected between ZO_2 and PMP22 [5]. PMP22 shares 28% amino acid homology with claudin-1 [11] but there is no YV motif in their C-termini (Fig. 1C).

3.2. Structural characterization of the binding groove in the ZO_2PDZ_1

We purified the ZO_2PDZ_1 for NMR studies. A set of unpublished data describing the ZO_2PDZ_1 solution 3D-structure is available in the Protein Database (PDB) (code: 2CSJ), which was used as a template during our analysis.

3.2.1. Backbone NMR resonance assignments for ZO_2PDZ_1

Backbone NMR chemical shift assignments for ZO_2PDZ_1 were completed based on standard 3-dimensional NMR experiments: HNCACB, CBCA(CO)NH, HNCA, HN(CO)CA, HNCO and HN(CA)CO. All backbone amides were assigned with the exception of the peaks from H37 and F38 (Fig. 2A), sites that resided in the long loop between β2 and β3 (Fig. 2B).

3.2.2. NMR-determined secondary structure of ZO_2PDZ_1

The secondary structure of ZO_2PDZ_1 was analyzed using the TALOS+ [14] based on backbone chemical shifts of ^{13}Ca, ^{13}CO and ^{15}NH. There were five β-strands (Glu7-Gln18, Ile27-Ser30, Ile45-Val50, Val66-Val69, and Ile92-Val103) and an α-helix (His79-Lys88) (Fig. 2B, C). This finding was consistent with the structural features of ZO_2PDZ_1 described in the unpublished structure of this protein by the Yokoyama group (PDB: 2CSJ). However, our study did not detect the short α-helix (Ala59-Leu62) seen in 2CSJ, which suggests reduced local stability in this region under the NMR conditions of this work.

3.2.3. Binding interface between the claudin-1 C-terminus (Cln1-C) and the ZO_2PDZ_1

The peptide Cln1-C (PSSGKDYV) was used to titrate ZO_2PDZ_1. Chemical shift perturbations by the peptide of the $^{1}H-^{15}N$ HSQC spectra allowed us to locate the peptide's binding site (Fig. 3A). Eight residues (Ile27, Gly26, Arg87, Leu51, Gly31, Leu78, Ser30, and Asp20) were deemed to be significantly perturbed based on chemical shift changes that were greater than one standard deviation above the mean (red arrows in Fig. 3A). The chemical shift changes for these sites were 0.80, 0.64, 0.55, 0.45, 0.35, 0.29, 0.27 and 0.22 ppm. A majority of the 8 peaks appeared to be in slow-to-intermediate exchange since peaks did not gradually shift from the free-state position to the fully bound position [15]. This feature was consistent with binding of moderately high affinity (low K_d value), as summarized in Table 1. Chemical shift changes ($\Delta\delta ppm$) of all backbone amide peaks between the free and bound state (0:1 to 1:6 peptide:protein ratio) were plotted as a function of residue number in Fig. 3B.

The results of the Cln1-C titration were examined in the context of the previously determined NMR structure of ZO_2PDZ_1 (PDB:2CSJ; unpublished) (Supplementary Fig. 2). The Cln1-C-perturbed residues were located in a pocket surrounded by a GFGI loop, equivalent to a previously described GLGF loop [8], which consisted of a β_B-β_C loop and an α_B/β_B groove (Supplementary Fig. 2A, B).

The overall structure of ZO_2PDZ_1 is similar to the PDZ_1 of ZO_1 [1,16]. We also verified the interaction between endogenous ZO_1 and claudin-1 in Schwann cells (Fig. 1E). This interaction depends on the C-terminus of claudin-1 [9]. These findings suggest that this interaction is conserved between ZO_1 and ZO_2; thus, subsequent experiments were conducted using only ZO_2.

3.3. The order of amino acids in the YV motif is essential for the interaction between the Cln1-C and the ZO_2PDZ_1

Deletion of the YV sites in the C-termini of claudins abolishes the binding between PDZ_1 of $ZO_1/ZO_2/ZO_3$ and claudin-1/claudin-2/claudin-3 [9]. To further explore how the YV-sequence plays roles in the binding, we performed titration experiments of ZO_2PDZ_1 with wild-type Cln1-C (PSSGKDYV) and mutant Cln1-C (Cln1-C-M1: PSSGKDAA or Cln1-C-M2: PSSGKDVY). The two mutants exhibited only minimal chemical shift perturbations in the $^{1}H-^{15}N$ HSQC spectrum even at a high peptide-to-protein ratio (Fig. 3C–F). In particular, changes in amino acids G26, I27 and R87 by the mutants were drastically decreased by 34-, 15- and 22-fold relative to those induced by the same concentration of wild-type Cln1-C (Fig. 3C–F; Table 1). These findings suggest that the interaction between Cln1-C and ZO_2PDZ_1 is strictly dependent on the YV motif.

3.4. The Y residue at the position −1 affects the binding affinity more strongly than the V residue at the position 0

To understand roles of C-terminal residues Y and V, titration experiments of ZO_2PDZ_1 with mutant Cln1-C-M3 (PSSGKDYA) or Cln1-C-M4 (PSSGKDAV) were performed. The binding affinity between ZO_2PDZ_1 and PSSGKDYA (Supplementary Fig. 1, Fig. 4A and C) was 4 times greater than that between ZO_2PDZ_1 and PSSGKDAV (Fig. 4B and D; Table 1). This finding suggests that the tyrosine side

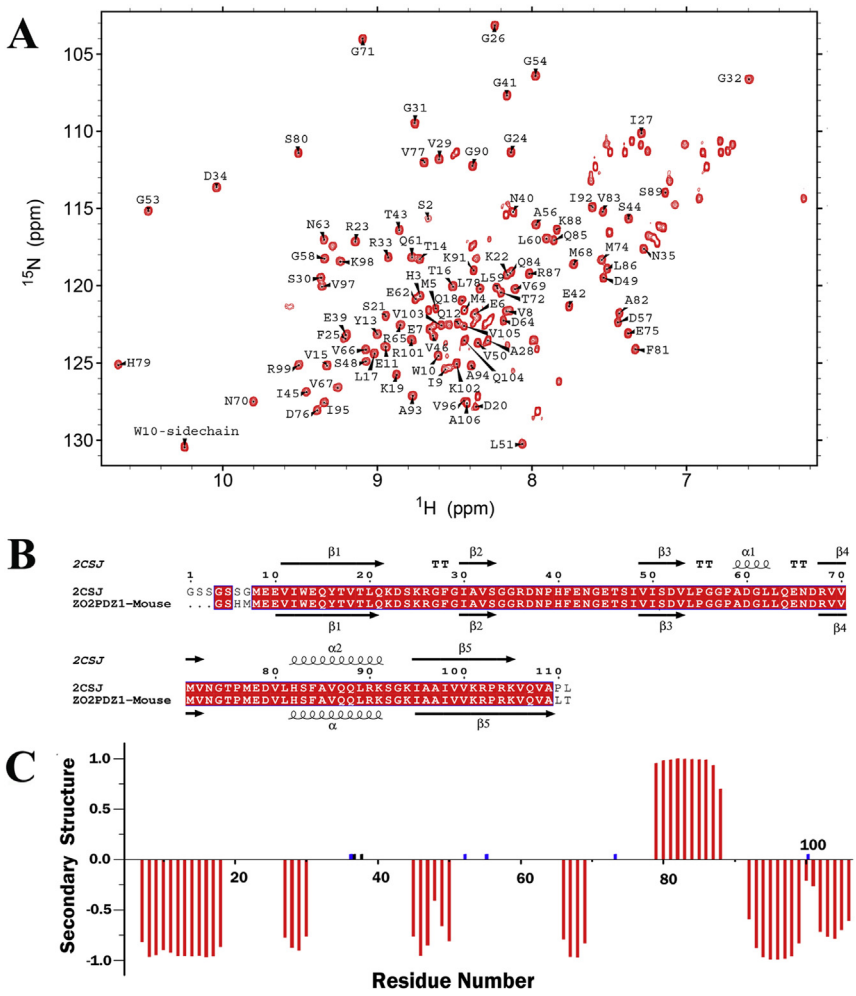

Fig. 2. Backbone assignment and secondary structure of mouse ZO_2PDZ_1. A. 600 MHz $^{1}H-^{15}N$ HSQC spectrum of the ZO_2PDZ_1 in pH 5.2 buffer at 25 °C. Assigned peaks are labeled with their residue numbers. **B**. Sequence alignment between the M-ZO_2PDZ_1 protein and the mouse ZO_2PDZ_1 in PDB:2CSJ using ClustalX and ESPript [3]. It confirms that residues of the ZO_2PDZ_1 were identical in the two sequences that are boxed by the large rectangular red background. Secondary structure elements seen in 2CSJ (unpublished data in PDB by Yokoyama and colleagues) are shown above the sequences with helices as squiggles, strands as arrows, and turns as TT. Notice that residue 1-7 and 110-111 were from the backbone DNA of the plasmids, and thus different between the two sequences. **C**. TALOS + analysis of the chemical shifts for the ZO_2PDZ_1. Positive value in Y-axis indicates α-helices, while the negative values indicate β-sheet. Unsigned peaks were marked by two small black bars. Prolines were indicated by small blue bars. Residues with an α- or β-propensity value near zero are not visible in the plot. (For interpretation of the references to color in this figure legend, the reader is referred to the web version of this article.)

chain at position −1 plays a critical role in the binding, whereas the side chain of valine at position 0 only exerts a lesser effect. This does not exclude a contribution from the terminal carboxyl group of the amino acid at position 0.

3.5. Amino acids at position −7 to −2 contribute minimally to the binding between claudin-1 C-terminus and ZO_2PDZ_1

To determine whether residues at position −7 to −2 play any significant roles in the binding between claudin-1 C-terminus and ZO_2PDZ_1, we took advantage of the native C-terminal peptide from PMP22. Our co-IP study failed to detect any interaction between ZO_2 and PMP22 (Supplementary Fig. 5 in Guo et al. Ann Neurol 2014) [5]. In line with this observation, only minimal changes of NMR chemical shifts were observed for ZO_2PDZ_1 upon titration by the wild type PMP22-C peptide that had an YV motif at its N-terminus, but not at its C-terminus (Supplementary Fig. 3A and B; Table 1). However, when the YV was relocated from the N-terminus (YVILRKRE, PMP22-C) to the C-terminus (PMP22-M1: ILRKREYV), the mutant PMP22-M1 induced large changes of chemical shifts for resonances from residues G26, I27, V29, L51 and R87. The binding affinity was comparable to that between ZO_2PDZ_1 and the Cln1-C (Supplementary Fig. 3C–D; Table 1). In contrast, both the wild-type YVILRKRE (Supplementary Fig. 3A, B) and mutant VYILRKRE were seen to be non-binders to ZO_2PDZ_1 (Supplementary Fig. 3E–F).

Taken together, while the residues from position −2 to −7 in PMP22-M1 differ from the corresponding residues in Cln1-C (Fig. 1C), PMP22-M1 still exhibited a binding affinity similar to that by Cln1-C (Table 1). This observation indicates that the residues between position −2 and −7 play no significant roles in determining the affinity of the binding between Cln1-C and ZO_2PDZ_1.

3.6. The myelin tight junction protein claudin-19 does not interact with ZO_2PDZ_1

Unlike the low levels of claudin-1/claudin-2/claudin-3/claudin-5 in myelinating Schwann cells, claudin-19 is highly enriched in tight junctions of myelin. Ablation of the *Claudin-19* gene completely eliminated myelin tight junctions in mouse peripheral nerves (16). In contrast to the YV-motif in the C-

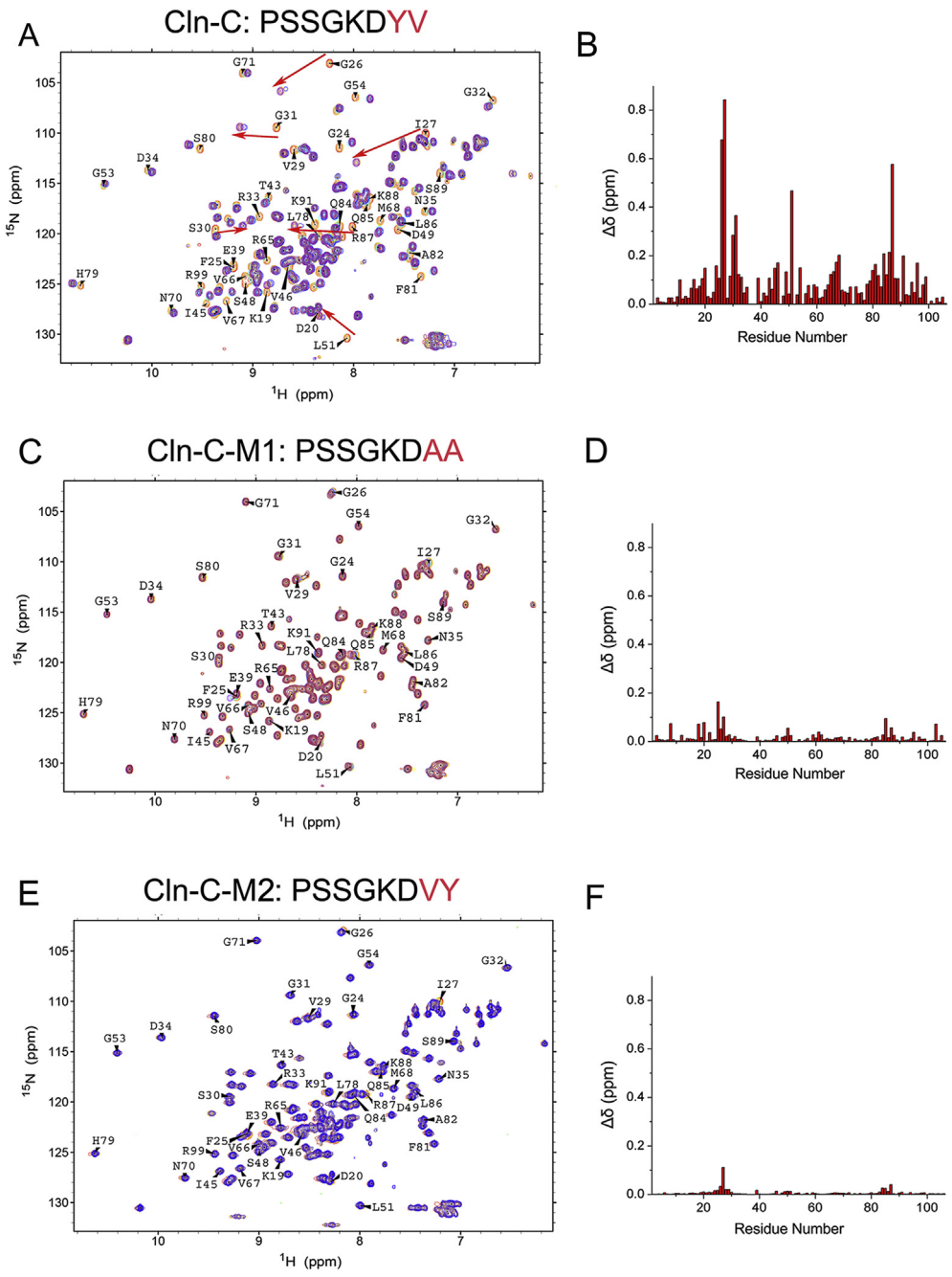

Fig. 3. Chemical shift perturbation of ZO_2PDZ_1 when titrated with Cln1-C (PSSGKDYV) and mutant-Cln1-C-M1, Cln1-C-M2 peptides (PSSGKDAA or PSSGKDVY). **A**. Superimposed $^{1}H-^{15}N$ HSQC spectra of ^{15}N-labeled ZO_2PDZ_1 in the absence and presence of Cln1-C. The peptide was titrated into the M-ZO_2PDZ_1 (50 mM peptide, 0.1 mM M-ZO_2PDZ_1 at pH5.2; the same conditions were used in the remaining figures and will not be repeated) up to 6 molar equivalents (in 8 steps) with ^{15}N-HSQC spectrum being acquired for each step (peptide to protein ratios 0:1, 1:8, 1:4, 1:2, 1:1, 2:1, 4:1, 6:1; colored in red, orange, maroon, purple, yellow, coral, pink, and blue). There were eight residues that showed significant changes of their chemical shifts in response to titration by Cln1-C. Other residues with chemical shift changes greater than the mean value were Lys19, Gly24, Val29, Gly32, Arg33, Glu39, Thr43, Ile45, Val46, Ile47, Ser48, Asp49, Gly54, Arg65, Val66, Val67, Met68, Ser80, Phe81, Ala82, Gln84, Gln85, Leu86, Lys88, Ser89, Lys91 and Arg99 (yellow bands). **B**. Histogram of the chemical shift perturbations in the presence of Cln1-C. **C**. Superimposed $^{1}H-^{15}N$ HSQC spectra of ^{15}N-labeled ZO_2PDZ_1 in the absence (black) and presence of mutant Cln1-C-M1 (PSSGKDAA) (titration points identical to those in A). **D**. Histogram of the chemical shift perturbations in the presence of PSSGKDAA. **E**. Superimposed $^{1}H-^{15}N$ HSQC spectra of ^{15}N-labeled ZO_2PDZ_1 in the absence and presence of Cln1-C-M2 (PSSGKDVY). The peptide was titrated into the ZO_2PDZ_1 up to 12 molar equivalents in 3 steps (Peptide:Protein ratios 0:1, 5:1, 8:1; 12:1; colored in red, yellow, pink, and blue). **F**. Histogram of the chemical shift perturbations in the presence of mutant Cln1-C-M2. (For interpretation of the references to color in this figure legend, the reader is referred to the web version of this article.)

termini of claudin-1-8 (4), a GV-motif is present in the C-terminus of claudin-19 (Fig. 1C). The GV-motif predicts a weak interaction between claudin-19 and ZO_2PDZ_1 since the residue at position −1 is not tyrosine. We performed NMR titration experiments using the C-terminal peptide of wild type claudin-19 (SVKGPLGV) and of a mutant (SVKGPLGA). Neither of the two peptides showed any binding to ZO_2PDZ_1 (Supplementary Fig. 4; Table 1). One might question whether the second and/or third PDZ domains in ZO_2 interact with claudin-19. We thus performed a co-IP experiment and found no interaction between full-length ZO_2 (including all three PDZ domains) and claudin-19 (Fig. 1D).

Table 1
List of NMR-determined K_d values for each peptide with ZO_2PDZ_1.

Peptide	Mutant	K_d (μM)
Cln1-C (-YV)	Wild type	45 ± 20
Cln1-C-AA	Cln1-C-M1	ND[1]
Cln1-C-VY	Cln1-C-M2	ND
Cln1-C-YA	Cln1-C-M3	500 ± 250
Cln1-C-AV	Cln1-C-M4	>2000
PMP22-C	Wild type	ND
PMP22-YV	PMP22-M1	150 ± 50
PMP22-VY	PMP22-M2	ND
MCT1-PV	Wild type	>2000
MCT1-PA	MCT1-C-M1	>2000
Cln-19-GV	Wild type	ND
Cln-19-GA	Cln19-C-M	ND

1. ND = not determined.

Finally, previous bioinformatics studies have predicted interactions between C-terminal motifs of many proteins and PDZ domains (17). For instance, monocarboxylate transporter-1 (MCT1; also known as SLC16A1) has a C-terminus (PTEEESPV) that is predicted to interact with PDZ domains. This protein has been suggested to play an important role in glia–axon interaction (18). However, our titration experiment showed only very weak interaction between the MCT1 C-terminus and ZO_2PDZ_1 (Supplementary Fig. 5A–B). Changing the "V" to "A" (MCT1-C-M1: PTEEESPA) further diminished binding (Supplementary Fig. 5C and D; Table 1). Thus, bioinformatics predictions need to be validated experimentally. Together, these findings provide further evidence that the residue Y at position −1 and, to a lesser degree, the V at residue 0, exerts the dominant role in the binding between claudins and ZO_1/ZO_2. Other residues in the C-terminus of claudins, appear to be much less important.

4. Discussion

Our study supports a critical role for the YV-motif in the interaction between PDZ_1 of ZO_1/ZO_2 and the C-termini of epi-/perineurial claudins. While the canonical model (involving non-ZO PDZ domains) emphasizes the dominant roles of the residue at the position 0 and −2 in the C-termini (17), our results suggest that interactions of ZO-derived PDZ domains with claudins in the PNS are different. Most notably, the latter interactions rely on the presence of a tyrosine at the position −1 for the binding of ZO and claudins. In light of the high similarity between ZO_1 and ZO_2 (4), the binding features observed for ZO_2/claudin interactions are expected to be applicable to the interactions between ZO_1 and claudins. This finding is significant for several reasons.

First, interactions between PDZ domains and their ligands have been extensively investigated. Results for non-ZO-derived PDZ have repeatedly confirmed important roles for the residues at the position 0 and −2. This canonical model has formed the molecular basis for drug development strategies for targeting PDZ-related interactions. This has proven to be fruitful in identifying compounds that modulate neurotransmitter-receptor binding. This approach has also led to successful discovery of small molecules that reduce the size of ischemic stroke in animal brains (19). However, our results suggest that the interactions between ZO_1/ZO_2 and epi/perineurial claudins have different molecular requirements from those in non-ZO PDZ/ligand interactions. Targeting interactions involving the residue at position −1 should be the focus of efforts to understand or disrupt interactions between the ZO_1/ZO_2 and epi/perineurial claudins. This notion is consistent with a previous study showing the dominant role of the residue at the position −1 in the interactions between the PDZ_1 of ZO_1 and an unspecified ligand (20).

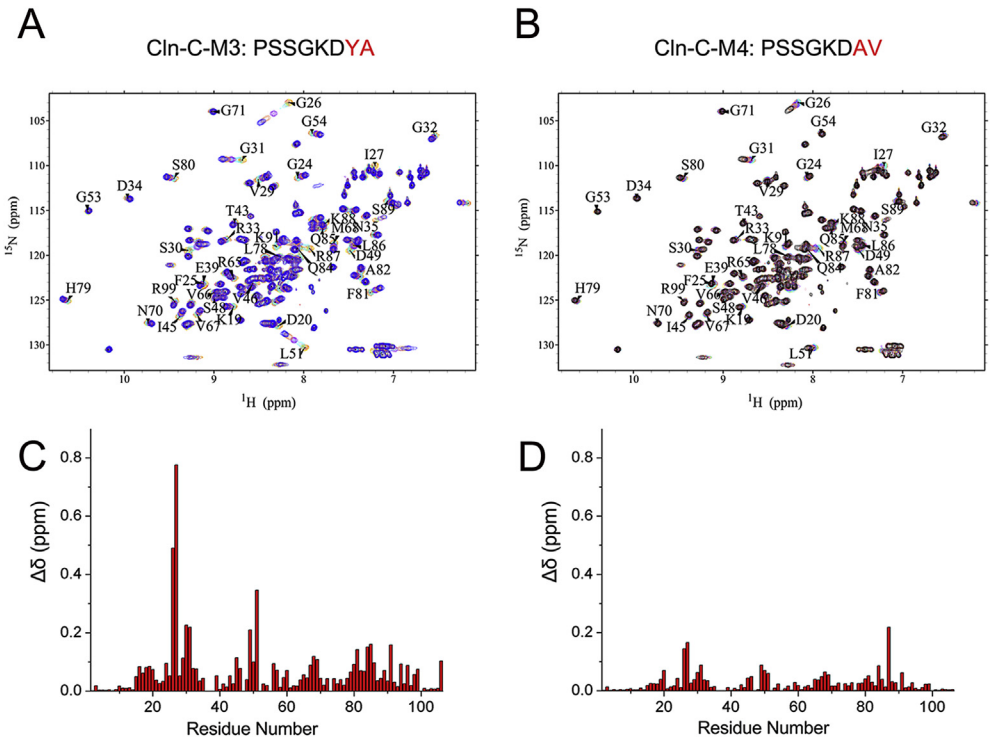

Fig. 4. Chemical shift perturbation of ZO_2PDZ_1 when titrated with Cln1-C-M3 (PSSGKDYA) and Cln1-C-M4 (PSSGKDAV). A. Superimposed ^{1}H–^{15}N HSQC spectra of ^{15}N-labeled ZO_2PDZ_1 in the absence and presence of Cln1-C-M3 (PSSGKDYA). The peptide was titrated into the ZO_2PDZ_1 up to 12 molar equivalents in 6 steps (Peptide:Protein ratios 0:1, 1:2, 1:1, 2:1, 4:1, 8:1, 12:1; colored in red, yellow, pink, cyan, purple, coral, and blue). **B**. Superimposed ^{1}H–^{15}N HSQC spectra of ^{15}N-labeled ZO_2PDZ_1 in the absence and presence of mutant Cln1-C-M4 (PSSGKDAV) (Peptide:Protein ratios 0:1, 1:2, 1:1, 2:1, 4:1, 8:1, 12:1; colored in red, yellow, pink, cyan, purple, coral, and black). **C&D**. Histogram of the chemical shift perturbations was generated in the presence of 12 molar equivalents Cln1-C-M3 (C) or Cln1-C-M4 peptide (D). (For interpretation of the references to color in this figure legend, the reader is referred to the web version of this article.)

The results of this work are also significant because interactions between ZO_1/ZO_2 and claudin-1/claudin-2 in the PNS have been suggested to play important roles in forming tight junctions of epi-/perineurium and rendering barriers against the entry of exogenous compounds. For example, application of hypertonic solutions to the PNS disrupts the epi-/perineurial tight junctions by decreasing expression of claudin-1. This disruption increases the entry of simultaneously administered analgesics to the PNS, which achieves better alleviation of pain (21). Our NMR experiments provide a promising platform that could be utilized to screen additional compounds [6] that may disrupt the epi-/perineurial tight junctions by targeting the interactions between PDZ_1 of ZO_1/ZO_2 and claudin-1/claudin-2/claudin-3/claudin-5.

In contrast to the tight junctions of epi-/perineurium, a different interaction mechanism must be utilized in the peripheral nerve myelin. Claudin-19 is highly enriched in peripheral nerve myelin, but not in the epi-/perineurium. Ablation of the *Claudin-19* gene eliminates tight junctions in peripheral nerve myelin, yet it results in only mild abnormalities in nerve conduction. The knockout mice (*Claudin-19−/−*) exhibits no obvious phenotype (16), even though mutations in human *Claudin-19* gene have been associated with renal diseases (23). This observation appears to be illuminated by our finding that shows no binding between the C-terminus of claudin-19 and the ZO_2PDZ_1 (Supplementary Fig. 4). While the deletion of *Claudin-19* eliminates tight junctions in myelin, the tight junctions formed by claudin-1/claudin-2 and ZO_1/ZO_2 in epi-/perineurium are independent of claudin-19 and still seal the peripheral nerve. However, when multiple types of junctions were simultaneously disrupted (tight junctions, adherens junctions and paranodal transmembrane adhesions) in PMP22-deficient peripheral nerves, both myelin and epi-/perineurium became highly permeable to exogenous molecules, resulting in impaired nerve conduction [5].

Claudin-3/claudin-5 express only minimally in the myelin of peripheral nerves (6), but are present at high levels in the peri-/epineurium (21). Because the C-termini of claudin-3/claudin-5 share the YV-motif identical to those in claudin-1/claudin-2 (Fig. 1C), claudin-3/claudin-5 should have a high binding affinity with the PDZ_1 of ZO_1/ZO_2. Thus, claudin-3/caludin-5 as well as claudin-1/claudin-2 are expected to play important role in the peri-/epineurial tight junctions. A small molecule targeting the binding between the C-termini of claudin-1/claudin-2/claudin-3/claudin-5 and ZO_1/ZO_2 would preferentially affect the epi-/perineurial tight junctions. The same drug would likely exert negligible effect against myelin tight junctions which mainly involve claudin-19, which does not interact with ZO_1/ZO_2 (Fig. 1 and Supplementary Fig. 4).

The overall structure of ZO_2PDZ_1 (see Supplementary Fig. 2) is similar to those observed for canonical PDZ domains (non-ZO PDZ-containing proteins) [10]. They are typically composed of 5–6 β-strands, a short α-helix (αA) and a long α-helix (αB). The canonical PDZ family has a highly conserved ligand-binding groove between the αB-helix and βB-strand. These shared structural features may not offer a direct explanation for the binding specificity of the PDZ_1 of ZO_1/ZO_2 for YV-terminated claudins. Additional studies will be required to establish the structural basis for how the ZO-derived PDZ_1 specifically recognize the side-chains and carboxyl terminal of the YV-motif.

In summary, our results demonstrate a dominant role of the residue at the position −1 in the binding between peripheral nerve claudins and the PDZ_1 of ZO_1/ZO_2. Small molecules targeting the interaction may differentially affect epi-/perineurial tight junctions from the tight junctions of the myelin. These findings may serve as important molecular basis for our future exploration of pharmaceutical interventions in the peripheral nerves.

Conflict of interest

None.

Acknowledgments

This research is supported by grants from NINDS (R21NS081364and R01NS066927 to J.L.) and VA R&D to J.L and by NIDDK RO1 DK083187 to C.R.S. The NMR instrumentation used in this work was supported by NIH S10 RR025677and by NSF DBI-0922862. This material is the result of work partially supported with resources and the use of facilities at the VA Tennessee Valley Healthcare System. This work does not necessarily reflect the views of the Department of Veterans Affairs.

Appendix A. Supplementary data

Supplementary data related to this article can be found at http://dx.doi.org/10.1016/j.bbrc.2015.02.075.

Transparency document

Transparency document related to this article can be found online at http://dx.doi.org/10.1016/j.bbrc.2015.02.075.

References

[1] B.A. Appleton, Y. Zhang, P. Wu, J.P. Yin, W. Hunziker, N.J. Skelton, S.S. Sidhu, C. Wiesmann, Comparative structural analysis of the Erbin PDZ domain and the first PDZ domain of ZO-1. Insights into determinants of PDZ domain specificity, J. Biol. Chem. 281 (2006) 22312–22320.
[2] F. Delaglio, S. Grzesiek, G.W. Vuister, G. Zhu, J. Pfeifer, A. Bax, NMRPipe: a multidimensional spectral processing system based on UNIX pipes, J. Biomol. NMR 6 (1995) 277–293.
[3] P. Gouet, E. Courcelle, D.I. Stuart, F. Metoz, ESPript: analysis of multiple sequence alignments in PostScript, Bioinformatics 15 (1999) 305–308.
[4] D. Grillo-Bosch, D. Choquet, M. Sainlos, Inhibition of PDZ domain-mediated interactions, Drug Discov. Today Technol. 10 (2013) e531–e540.
[5] J. Guo, L. Wang, Y. Zhang, J. Wu, S. Arpag, B. Hu, B.A. Imhof, X. Tian, B.D. Carter, U. Suter, J. Li, Abnormal junctions and permeability of myelin in PMP22-deficient nerves, Ann. Neurol. 75 (2014) 255–265.
[6] M.J. Harner, A.O. Frank, S.W. Fesik, Fragment-based drug discovery using NMR spectroscopy, J. Biomol. NMR 56 (2013) 65–75.
[7] A. Hartsock, W.J. Nelson, Adherens and tight junctions: structure, function and connections to the actin cytoskeleton, Biochim.Biophys. Acta 1778 (2008) 660–669.
[8] B.J. Hillier, K.S. Christopherson, K.E. Prehoda, D.S. Bredt, W.A. Lim, Unexpected modes of PDZ domain scaffolding revealed by structure of nNOS-syntrophin complex, Science 284 (1999) 812–815.
[9] M. Itoh, M. Furuse, K. Morita, K. Kubota, M. Saitou, S. Tsukita, Direct binding of three tight junction-associated MAGUKs, ZO-1, ZO-2, and ZO-3, with the COOH termini of claudins, J. Cell Biol. 147 (1999) 1351–1363.
[10] H.J. Lee, J.J. Zheng, PDZ domains and their binding partners: structure, specificity, and modification, Cell. Commun.Signal 8 (2010) 8.
[11] L. Notterpek, K.J. Roux, S.A. Amici, A. Yazdanpour, C. Rahner, B.S. Fletcher, Peripheral myelin protein 22 is a constituent of intercellular junctions in epithelia, Proc. Natl. Acad. Sci. U.S.A 98 (2001) 14404–14409.
[12] S. Poliak, S. Matlis, C. Ullmer, S.S. Scherer, E. Peles, Distinct claudins and associated PDZ proteins form different autotypic tight junctions in myelinating Schwann cells, J. Cell Biol. 159 (2002) 361–372.
[13] K.P. Pummi, A.M. Heape, R.A. Grenman, J.T. Peltonen, S.A. Peltonen, Tight junction proteins ZO-1, occludin, and claudins in developing and adult human perineurium, J. Histochem. Cytochem. 52 (2004) 1037–1046.
[14] Y. Shen, F. Delaglio, G. Cornilescu, A. Bax, TALOS+: a hybrid method for predicting protein backbone torsion angles from NMR chemical shifts, J. Biomol. NMR 44 (2009) 213–223.
[15] I.O. Sutherland, Investigation of the kinetics of conformational changes by nuclear magnetic resonance spectroscopy, in: E.F. Mooney (Ed.), Academic Press Inc., New York City, 1971, pp. 71–235.
[16] Y. Umetsu, N. Goda, R. Taniguchi, K. Satomura, T. Ikegami, M. Furuse, H. Hiroaki, 1H, 13C, and 15N resonance assignment of the first PDZ domain of mouse ZO-1, Biomol.NMR Assign. 5 (2011) 207–210.
[17] R.A. Williamson, M.D. Carr, T.A. Frenkiel, J. Feeney, R.B. Freedman, Mapping the binding site for matrix metalloproteinase on the N-terminal domain of the tissue inhibitor of metalloproteinases-2 by NMR chemical shift perturbation, Biochemistry 36 (1997) 13882–13889.